# *Ab initio* calculation of the giant magnetostriction in terbium and erbium

S. Buck and M. Fähnle

*Max-Planck-Institut für Metallforschung, Heisenbergstraße 1, D-70569 Stuttgart, Germany*

(Received 4 February 1998)

The single-ion $4f$ contributions to the components $\lambda_2^{\alpha,2}$, $\lambda^{\gamma,2}$, and $\lambda_1^{\alpha,2}$ of the giant magnetostriction tensor of Tb and Er are calculated *ab initio* by a constrained density-functional theory in the local spin-density approximation and the full-potential linear-muffin-tin-orbital method. The data exhibit the expected change in sign when going from Tb with an oblate $4f$ charge density to Er with a prolate $4f$ charge density. The satisfactory agreement with experimental results shows that the giant magnetostriction in Tb and Er is dominated by the single-ion $4f$ contribution. [S0163-1829(98)50722-9]

The anisotropic magnetostriction, i.e., the change of the shape of a magnet caused by the modification of the size and/or direction of the magnetic moment, plays an important role for technological applications. For electric transformers or motors or magnetic shielding, etc., soft magnetic materials with extremely small magnetostrictive strains (typically several $10^{-6}$) are required.[1] In contrast, materials with large magnetostrictive strains are used in many electromagnetic micro devices,[1] such as actuators and sensors. The largest magnetostrictive strains (up to about $10^{-2}$) were found in elementary rare-earth metals,[2] albeit only at low temperatures (because of the low Curie temperatures $T_C$) and in high magnetic fields (because of the large magnetocrystalline anisotropy). The anisotropy may be reduced by combining several rare-earth atoms, and $T_C$ may be increased by the addition of transition-metal atoms, arriving at alloys of rare-earth atoms and transition-metal atoms which exhibit magnetostrictive strains of about $10^{-3}$ at room temperature and moderate magnetic fields.[1,3]

Among the various possible sources[1] for magnetocrystalline anisotropy and magnetostriction the spin-orbit coupling is the most important one. In transition metals the electrons which are responsible for magnetism are itinerant and the spin-orbit coupling is very weak and can be treated using a perturbative framework. Most recently, the magnetostriction in bulk fcc Co and in thin Co films has been calculated *ab initio* by such a perturbative approach.[4] In contrast, in most rare-earth metals the $4f$ electrons dominate the magnetic behavior, and these are well localized and exhibit very large intra-atomic couplings, with a $4f$ spin-orbit coupling which is often considerably larger than the anisotropic part of the couplings between the $4f$ electrons and all the other charges in the system.[5] As a consequence, the $4f$ system is often treated as a system with infinite spin-orbit coupling: When the orientation of the magnetic moment of the $4f$ shell is rotated against the crystallographic axes by the application of a very strong external magnetic field, it is assumed that the anisotropic $4f$ charge density is rigidly corotated. Thereby the interaction energy of the $4f$ electrons with the surrounding charges increases, and this is the physical origin of the large magnetocrystalline anisotropy energy (see Ref. 5 and references therein). Furthermore, the atoms surrounding the $4f$ shell will attain new equilibrium positions when changing the orientation of the anisotropic $4f$ charge density in order

to minimize the total energy, and this will result in magnetostrictive strains. The present paper represents an *ab initio* calculation of this single-ion $4f$-induced magnetostriction. We thereby consider the elementary hexagonal close-packed rare-earth metals Tb and Er because of the following reasons. First, the magnetostrictive strains are very large in both materials. Second, the $4f$ charge density of Tb is oblate, whereas the one of Er is prolate. When going from Tb to Er we therefore expect a change in the sign of magnetostrictive strains. Third, in Tb and Er the $4f$ states are well localized, and most features may be described by treating them as true core states. Finally, in all heavy rare earths but Gd the two-ion contributions to anisotropy and saturation magnetostriction are much smaller than the single-ion spin-orbit contribution which—in turn—is dominated by the $4f$ contribution.[6]

In hexagonal materials there are six independent components of the magnetostriction tensor,[7] which describe the change $\Delta l$ in the linear extension of a crystal relative to the length $l$ of a nonmagnetic reference state in the direction given by the direction cosines $\beta$ when the magnetization is switched on in a direction described by the direction cosines $\alpha$:

$$
\frac{\Delta l}{l}\bigg|_{\alpha,\beta} = \left[\lambda_1^{\alpha,0} + \lambda_1^{\alpha,2}\left(\alpha_z^2 - \frac{1}{3}\right)\right](\beta_x^2 + \beta_y^2)
$$

$$
+ \left[\lambda_2^{\alpha,0} + \lambda_2^{\alpha,2}\left(\alpha_z^2 - \frac{1}{3}\right)\right]\beta_z^2
$$

$$
+ \frac{1}{2}\lambda^{\gamma,2}[(\alpha_x\beta_x + \alpha_y\beta_y)^2 - (\alpha_x\beta_y - \alpha_y\beta_x)^2]
$$

$$
+ 2\lambda^{\epsilon,2}(\alpha_x\beta_x + \alpha_y\beta_y)\alpha_z\beta_z. \tag{1}
$$

In the present paper we determine the lengths of the axes $a$, $b$, and $c$ (Fig. 1) for an orientation of the magnetostriction along the $c$ axis and along the $b$ axis, respectively. From these data we can calculate the components $\lambda_2^{\alpha,2}$, $\lambda^{\gamma,2}$, and $\lambda_1^{\alpha,2}$, for which Eq. (1) yields in a linear approximation
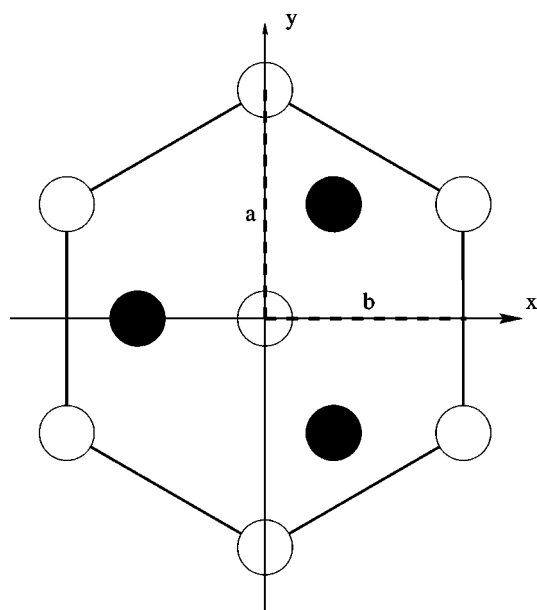
$$
\lambda_2^{\alpha,2} = \frac{c_c - c_b}{c_b}, \tag{2}
$$

FIG. 1. Projection of the atoms in the basal plane $A(x\text{-}y)$ of the hexagonal system. The black atoms are the atoms of the $B$ layer located at a distance of $c/2$ above the basal plane.

$$\lambda^{\gamma,2} = 2\,\frac{\epsilon - \dfrac{\sqrt{3}}{2}}{\epsilon + \dfrac{\sqrt{3}}{2}}, \qquad (3)$$

$$\lambda_1^{\alpha,2} = \frac{b_c}{b_b} - 1 + \frac{1}{2}\lambda^{\gamma,2}. \qquad (4)$$

Here $c_c(c_b)$ denotes the length of the crystallographic $c$ axis when the $4f$ magnetic moments are aligned to the $c$ axis ($b$ axis) and $\epsilon = b/a$ is the ratio of the lengths of the $b$ axis and the $a$ axis when the $4f$ moments are aligned to the $b$ axis. (For the definitions of the axes see Fig. 1). For this latter orientation, the symmetry of the crystal is orthorhombic due to the distortion of the basal plane. In addition, it has to be taken into account that for this orthorhombic unit cell there is an internal degree of freedom, namely, the second layer B of the stacking sequence . . . ABAB . . . , which is located at a distance of $c/2$ above the basal plane A (Fig. 1), may rigidly move into the direction of the $4f$ moments by a distance $\delta$. Hence, there are two structural parameters $(a, c/a)$ or four structural parameters $(a,\ c/a,\ \epsilon,\ \text{and}\ \delta)$ which must be determined by minimizing the total energy for the orientation of the $4f$ moments along the $c$ axis or along the $b$ axis, respectively. The minimization was performed in an iterative way: First, the parameters $a_c$ and $c_c/a_c$ are determined for an orientation of the $4f$ moments along the $c$ axis (hexagonal unit cell). Then the $4f$ moments are aligned along the $b$ axis, and $c_b$ is determined while fixing the hexagonal crystal structure $(\epsilon = \sqrt{3}/2,\ \delta = 0)$. In the next step we allow for an orthorhombic distortion of the unit cell and determine $a_b$, $\epsilon$, and $\delta$ for fixed $c_b$. At the end, the final values of $a_b$ and $c_b$ are obtained while fixing $\epsilon$ and $\delta$. It should be noted that $\delta$ is very small (some $10^{-2}$ a.u.) and that the influence of the magnetostriction in the basal plane on $c_b$ is also very small

(i.e., $c_b$ attains nearly the same values for hexagonal ($\epsilon = \sqrt{3}/2$) or orthorhombic ($\epsilon \neq \sqrt{3}/2$) structure of the basal plane).

For the structural optimization the total energy is determined *ab initio* within the framework of the spin-density functional theory in local-spin-density approximation (LSDA), with the exchange-correlation functional of Moruzzi *et al.*[8] Because the change of the energy resulting from the magnetostrictive deformation is very small, all electronic states (i.e., $4f$ states, non-$4f$ core states, and valence states) must be treated with very high accuracy.

$4f$ *states:* For a description of the $4f$ states we adopt the extreme version of the standard model of rare-earth magnetism (see, e.g., Ref. 5) which assumes that the intra-atomic Hund's rule couplings in the $4f$ shell of the trivalent rare-earth atoms in the metal are so strong that the $4f$ charge and spin density is not affected by the interaction with all the other charges in the system. Indeed, the neutron magnetic form factors of the $4f$ spin density in metallic Gd[9] and Er[10] agree very well with those calculated for the free Gd$^{3+}$ and Er$^{3+}$ ions by a fully relativistic Dirac-Fock study,[11] indicating that in these cases the metallic environment does not matter. The $4f$ states themselves cannot be described correctly by the LSDA, but we assume that the interaction between the $4f$ states and the other states which induces the magnetostriction is well represented by this approximation. Because in spin-density functional theory the electronic ground-state energy is totally determined by the spin and charge densities, we could in principle straightforwardly insert the $4f$ spin and charge densities obtained by the Dirac-Fock calculations for the free rare-earth ions. As we do not have the Dirac-Fock program at hand, we model the $4f$ charge and spin density according to Eqs. (16)–(19) from Ref. 5. In this prescription the correct angular dependences are reproduced, and realistic radial dependences are obtained by a constrained LSDA: The $4f$ single-particle eigenfunctions are obtained by solving the Kohn-Sham equations for the spherically averaged effective potential of the crystal, thereby applying the boundary condition that the wave function is zero at the surface of a localization sphere. The radius of this sphere is chosen in such a way that the moments $\langle r^n \rangle_{4f}$ for $n = 2,4,6$ match the corresponding moments of the Dirac-Fock calculation[11] for the free trivalent rare-earth ion as closely as possible. To stay within the framework of the standard model this localization sphere is kept constant during the structural optimization. It should be noted that—alternatively—realistic $4f$ radial dependences can be obtained by applying the self-interaction correction.[12]

*Non-$4f$ core states:* The non-$4f$ core states feel the asphericity of the surrounding charge densities and of the $4f$ core and therefore experience an aspherical distortion which may contribute to the magnetostriction. This was taken into account by applying a scalar-relativistic version[13] of the effective-potential method for the calculation of the electronic core polarization,[14] in which the Kohn-Sham equation for the core states in the aspherical effective potential is solved with a basis set which is composed of the respective solutions in the spherical part of the effective potential and of Gaussians with different widths. Test calculations have shown that for Tb and Er this effect of the core polarization

TABLE I. The components $\lambda_2^{\alpha,2}$ and $\lambda^{\gamma,2}$ of the magnetostriction in Tb and Er. The value with the asterisk has been extrapolated from Fig. 7 of Ref. 21.

| | $\lambda_2^{\alpha,2}[10^{-2}]$ | $\lambda^{\gamma,2}[10^{-2}]$ | |
|---|---|---|---|
| | $1.71\pm0.1$ | $1.00\pm0.09$ | this paper |
| | – | $0.87^{6}$ | directly measured |
| | – | $0.67^{21}$ | |
| Tb | $0.90^{6}$ | – | extrapolated from |
| | $0.90^{17}$ | $1.0^{17}$ | the paramagnetic |
| | $1.5^{18}$ | $0.85^{18}$ | regime |
| | $1.45^{20}$ | $0.68^{20}$ | extrapolated from |
| | $0.97^{21}*$ | $0.67^{21}$ | diluted systems |
| | $-0.41\pm0.1$ | $-0.47\pm0.11$ | this paper |
| | – | $-0.54^{22}$ | extrapolated from the |
| Er | | | paramagnetic regime |
| | $-0.59^{20}$ | $-0.59^{20}$ | extrapolated from |
| | | | diluted systems |

on the magnetostriction is small (about 10%) so that the core polarization effect was neglected in the final calculations.

*Valence states:* The valence states are nonspherical, because they feel the crystal symmetry as well as the asphericity of the $4f$ core. It has been shown[15] that the $4f$-induced asphericity of the valence states is of the same order of magnitude as the one due to the aspherical crystal potential. For an accurate description of the valence states the full-potential linear-muffin-tin-orbital method developed in Ref. 5 and based on an original code of Savrasov and Savrasov[16] was applied. A set of basis functions according to three different kinetic energy parameters $\kappa^2$ was used, whereby one $\kappa^2$ is required to include the high-lying $5p$ states of the rare-earth atom into the band calculation. The $5s$ states are treated as semicore states. For details, see Ref. 5. Test calculations have shown that the results for $\lambda_2^{\alpha,2}$ change by only 10% when using only two $\kappa^2$ values, but the absolute values of $c_b$ and $c_c$ change rather drastically. It turned out that the choice of various muffin-tin radii (fixed radii vs variable and always touching radii) modifies the magnetostriction results by only (5–10)%, and fixed muffin-tin radii were used for the final calculations.

Table I shows the numerical results for $\lambda_2^{\alpha,2}$ and $\lambda^{\gamma,2}$, and a comparison with experimental data. The error limits of our data include only the contributions arising from the finite number of total energy calculations for the structural optimi-

zation. The experimental determination of the zero-temperature components of the magnetostriction tensor is hampered by the large magnetic anisotropy which does not allow to rotate the magnetization completely in any required crystallographic direction by application of the available magnetic fields. Therefore, for Tb and Er the only component which has been obtained by a direct measurement[2] at $T=0$ K is $\lambda^{\gamma,2}$ of Tb, because in this material the $b$ axis is the easy axis and rotation to the $a$ axis requires only moderate fields. The other components have to be determined by extrapolating the magnetostriction data in the paramagnetic regime[2,17,18] to zero temperature by means of the single-ion theory of Callen and Callen,[19] or they are estimated by extrapolating the low-temperature results for the magnetoelastic coefficients in diluted $\underline{Y}$Tb and $\underline{Gd}$Tb alloys to a concentration of 100% rare earth.[20,21] For Er a further complication arises, because it exhibits[22] a conical ferromagnetic structure around the $c$ axis at low temperatures which is modified by the application of a strong field. Here the zero temperature components of the saturation magnetostriction tensor (i.e., the components which would arise for perfect ferromagnetic alignment) have been obtained by extrapolating the magnetostriction data in the paramagnetic regime to zero temperature,[22] or by extrapolating the low temperature results for diluted $\underline{Y}$Er alloys to a concentration of 100% rare earth.[20] It becomes obvious from Table I that in view of the large experimental uncertainties the agreement between theory and experiment is satisfactory. This confirms from a theoretical point of view that the single-ion $4f$ contribution is indeed the dominant contribution to the saturation magnetostriction in Tb and Er.

The calculation of $\lambda_1^{\alpha,2}$ is numerically very delicate, because according to Eq. (4) $\lambda_1^{\alpha,2}$ is given by the sum of two small terms ($b_c/b_b-1$ and $\frac{1}{2}\lambda^{\gamma,2}$) with opposite sign. We obtained $\lambda_1^{\alpha,2}=(-0.75\pm0.24)\times10^{-2}$ for Tb and $(0.23\pm0.20)\times10^{-2}$ for Er, where the error limits again include only the contributions arising from the finite number of total energy calculations for the structural optimization. The experimental results exhibit a large scatter. DeSavage and Clark[17] obtained $\lambda_1^{\alpha,2}=-0.26\times10^{-2}$ for the Tb metal by extrapolating from the paramagnetic regime to zero temperature, whereas the data of Chaudhri *et al.*[21] for diluted $\underline{Gd}$Tb systems extrapolated to pure Tb would yield $\lambda_1^{\alpha,2}=-0.48\times10^{-2}$. Curiously enough, Pureur *et al.*[20] extrapolated their data for extremely diluted $\underline{Y}$Tb and $\underline{Y}$Er systems to a positive value of $\lambda_1^{\alpha,2}(0.88^{+0.38}_{-0.88}\times10^{-2})$ for pure Tb and a negative value $(-0.29^{+0.29}_{-0.09}\times10^{-2})$ for pure Er.

[1] E. du Trémolet de Lacheisserie, *Magnetostriction: Theory and Applications of Magnetoelasticity* (CRC Press, Boca Raton, 1993).

[2] J. J. Rhyne and S. Legvold, Phys. Rev. **138**, A507 (1965).

[3] A. E. Clark and H. S. Belson, AIP Conf. Proc. **10**, 749 (1972).

[4] R. Wu and A. J. Freeman, J. Appl. Phys. **79**, 6209 (1996).

[5] K. Hummler and M. Fähnle, Phys. Rev. B **53**, 3272 (1996).

[6] J. J. Rhyne, in *Magnetic Properties of Rare Earth Metals*, edited by R. J. Elliott (Plenum Press, London 1972), Chap. 4.

[7] R. R. Birss, *Symmetry and Magnetism* (North-Holland, Amsterdam, 1966).

[8] V. L. Moruzzi, J. F. Janak, and A. R. Williams, *Calculated Electronic Properties of Metals* (Pergamon, New York, 1978).

[9] R. M. Moon, W. C. Koehler, J. W. Cable, and H. R. Child, Phys. Rev. B **5**, 997 (1972).

[10] C. Stassis, G. R. Kline, A. J. Freeman, and J. P. Desclaux, Phys. Rev. B **13**, 3916 (1976).

[11] A. J. Freeman and J. P. Desclaux, J. Magn. Magn. Mater. **12**, 11 (1979).

[12] L. Steinbeck, M. Richter, U. Nitzsche, and H. Eschrig, Phys. Rev. B **53**, 7111 (1996).

[13] O. Grotheer, S. Buck, and M. Fähnle (unpublished).

[14] J. Ehmann and M. Fähnle, Phys. Rev. B **55**, 7478 (1997).

[15] S. Buck and M. Fähnle, J. Magn. Magn. Mater. **166**, 297 (1997).

[16] S. Yu. Savrasov and D. Yu. Savrasov, Phys. Rev. B **46**, 12 181 (1992).

[17] B. F. DeSavage and A. E. Clark, in *Magnetic Properties of Rare Earth Metals* (Ref. 6).

[18] P. de V. du Plessis, Philos. Mag. **18**, 145 (1968).

[19] E. R. Callen and H. B. Callen, Phys. Rev. **129**, 578 (1963).

[20] P. Pureur, G. Creuzet, and A. Fert, J. Magn. Magn. Mater. **53**, 121 (1985).

[21] M. A. Chaudhri, W. D. Corner, and A. A. Joraide, J. Magn. Magn. Mater. **65**, 53 (1987).

[22] J. J. Rhyne and S. Legvold, Phys. Rev. **140**, A2143 (1965).